

## Sympathetic Cooling of Complex Molecular Ions to Millikelvin Temperatures

A. Ostendorf, C. B. Zhang, M. A. Wilson, D. Offenberg, B. Roth, and S. Schiller

*Institut für Experimentalphysik, Heinrich-Heine-Universität Düsseldorf, 40225 Düsseldorf, Germany*

(Received 14 July 2006; published 15 December 2006)

Gas-phase singly protonated organic molecules of mass 410 Da (Alexa Fluor 350) have been cooled from ambient temperature to the hundred millikelvin range by Coulomb interaction with laser-cooled barium ions. The molecules were generated by an electrospray ionization source, transferred to and stored in a radio-frequency trap together with the atomic ions. Observations are well described by molecular dynamics simulations, which are used to determine the spatial distribution and thermal energy of the molecules. In one example, an ensemble of 830 laser-cooled  $^{138}\text{Ba}^+$  ions cooled 200 molecular ions to less than 115 mK. The demonstrated technique should allow a large variety of protonated molecules to be sympathetically cooled, including molecules of much higher mass, such as proteins.

DOI: [10.1103/PhysRevLett.97.243005](https://doi.org/10.1103/PhysRevLett.97.243005)

PACS numbers: 33.80.Ps, 32.80.Lg, 42.50.Vk, 47.11.Mn

One of the current themes of quantum physics is the creation of cold ( $<1$  K) molecules to study molecule-molecule, molecule-atom, and molecule-radiation interactions under these novel low temperature conditions. The recent progress in this field has seen the development of methods for cooling and simultaneously confining molecules using external fields. So far, the production of cold molecules has been limited to few-atom molecules. Neutral di-, tri-, and tetra-atomic molecules can be produced by atom-to-molecule conversion methods in ultra-cold atomic gases [1]. Cold magnetic few-atom molecules have been produced by buffer gas cooling in a magnetic trap [2]; slow molecules with electric dipole moments have been produced by Stark deceleration [3] and by cold particle selection, and trapped in electric traps [4]. Molecules can be implanted into superfluid droplets of  $^3\text{He}$  and  $^4\text{He}$ , and acquiring the droplet temperature ( $T \approx 0.38$  K) [5]. Sympathetic cooling [6,7] has been used to cool charged diatomic and triatomic molecules to tens of mK by Coulomb interaction with laser-cooled atomic ions in radio-frequency ion traps [8–10]. This approach has recently enabled high-resolution ro-vibrational spectroscopy of molecular ions at sub-Kelvin temperature [11].

There is need for methods to permit a similar control over complex, i.e., massive, molecules. Here we demonstrate a significant extension of the mass range of molecules that can be prepared at low temperatures in the gas phase, demonstrating, for the first time to our knowledge, cooling of stored polyatomic molecules (containing 42 atoms in this case) to a temperature range significantly below that reachable with conventional cryogenic techniques (buffer gas cooling, typically at  $\sim 10$  K) [12], or in previous sympathetic cooling ( $\sim 14$  K) [13]. Our method furthermore allows strong spatial localization of the molecules. The source type employed, electrospray ionization [14], is commonly used for mass spectroscopy of macromolecules and can be used to produce a vast variety of protonated molecular ions in various charge states and, in particular, molecular ions of biological interest (e.g., proteins). We expect that the cooling method

demonstrated here can be extended to such large molecules as well, leading to new approaches for studies of biomolecular systems. Since the cooling method used is independent of the internal structure of the ions it is not limited to molecules, but could also be used with atomic or other clusters.

The apparatus consists of an electrospray molecular ion source (ESI), an octopole ion guide transporting the ions into a linear rf trap, a barium ion source, an ion counter, a fluorescence detector and an intensified CCD camera for observing the barium ions, and a laser system for Doppler cooling. Except for the last three, these parts are enclosed in a vacuum chamber, in which the pressure drops from atmospheric pressure at the ion source to  $5 \times 10^{-10}$  mbar in the trap region. Molecular compounds are dissolved in a solution which is injected into the ESI source. There, charged droplets of the solvent are ejected by a needle and undergo rapid evaporation into smaller and smaller droplets until a final Coulomb explosion causes a significant fraction of single molecules to be created with varying numbers of protons attached. Molecules of a desired charge-to-mass ratio are then selected using a quadrupole mass filter (resolution 1 Da). The rf octopole ion guide channels the molecules to the trap. It is 1.9 m long and collinear with the trap axis.

The linear quadrupole trap produces an effective trap potential with radial dependence  $(QV_0/\Omega r_0)^2(r/r_0)^2/4m$ , where  $Q$  is the ion charge,  $m$  is the mass,  $\Omega = 2\pi \times 2.5$  MHz is the trap rf frequency,  $V_0/2 = 200$  V is the rf amplitude applied to each electrode, and  $r$  is the radial distance from the trap ( $z$ ) axis ( $r_0 = 4.4$  mm is the axis-to-electrode-surface distance). Thus, heavier ions experience a shallower trapping potential. In this potential, the ions can oscillate, with a mass-to-charge-ratio-dependent characteristic frequency. This secular oscillation can be excited by applying an ac voltage to the trap electrodes.

The loading and laser-cooling of the barium ions is described in [10]. Cold barium ion ensembles are routinely produced by Doppler cooling. The final steady-state ki-

netic energy per particle is so low that the interparticle Coulomb repulsion energy dominates, leading to structured ensembles [15,16]. They vary in shape from linear strings to large ‘‘Coulomb crystals’’ composed of spheroidal shells, depending on the total ion number and the chosen trap parameters. Crystals as cold as 5 mK have been observed and typical ion-ion distances are around 25  $\mu\text{m}$ . At the lowest temperatures discrete ‘‘sites’’ in the crystals become apparent.

We have used the molecular compound Alexa Fluor 350 ( $\text{C}_{16}\text{H}_{14}\text{N}_2\text{O}_9\text{S}$ ) (herein denoted by AF), since its peak absorption wavelength around 350 nm makes it stable against photodissociation by the 493 and 650 nm cooling lasers [17]. The compound is dissolved in a 50:50 solution of methanol and water at a concentration of 250 pmol/ml. Formic acid is added at 1.25% concentration to protonate the AF molecules. Singly protonated  $\text{AF}^+$  ions were then selected using the mass filter, as higher charge states were less abundant for this molecule.

The following procedure for producing sympathetically cooled ensembles of  $\text{AF}^+$  molecules was developed. First, helium buffer gas was injected into the trap chamber via a leak valve to a pressure of  $1 \times 10^{-4}$  mbar and  $\text{AF}^+$  was loaded into the trap for 6 s. The room-temperature buffer gas serves to efficiently remove the high kinetic energy of the incoming molecular ions and cool them to  $\sim 300$  K. The buffer gas was then rapidly pumped away with the background pressure returning to the  $10^{-10}$  mbar level a few minutes later. Next, a cloud of barium ions was loaded from the oven into the trap. Lighter impurity ions generated at the same time were ejected from the trap by applying a strong swept-frequency (125–500 kHz) secular excitation. In this way a cold crystal of barium ions was obtained, surrounded by heavier  $\text{AF}^+$  ions [Fig. 1(a) and 1(b)]. The laser-cooled barium crystal acts to sympathetically cool the  $\text{AF}^+$  ions and, conversely, the presence of the  $\text{AF}^+$  slightly heats the barium ensemble. The sympathetically cooled barium isotopes lie on the right-hand side of the crystal due to light pressure forces pushing the  $^{138}\text{Ba}^+$  ions to the left [Fig. 1(a)]. This particular two-species ensemble was trapped and cooled for 4 minutes, but this time could be as long as an hour.

The trap contents can be determined using a nondestructive and a destructive technique. Resonant secular excitation of a particular species leads to a drop in the  $^{138}\text{Ba}^+$  fluorescence rate because the coolant ions are heated, either directly or through interspecies interactions. Radial resonances were observed at typically 102 kHz (for direct  $\text{Ba}^+$  excitation) and at around 33 kHz (Fig. 2). The latter value implies a mass of the trapped molecules of  $418 \pm 11$  amu, consistent with the value expected for  $\text{AF}^+$ . The excitation amplitude used heated the ensemble so strongly that the crystal melted. When scanning from high to low frequency this permitted the measurement of the single-particle secular frequency as opposed to the (shifted) frequency of a strongly coupled two-component crystal [18].

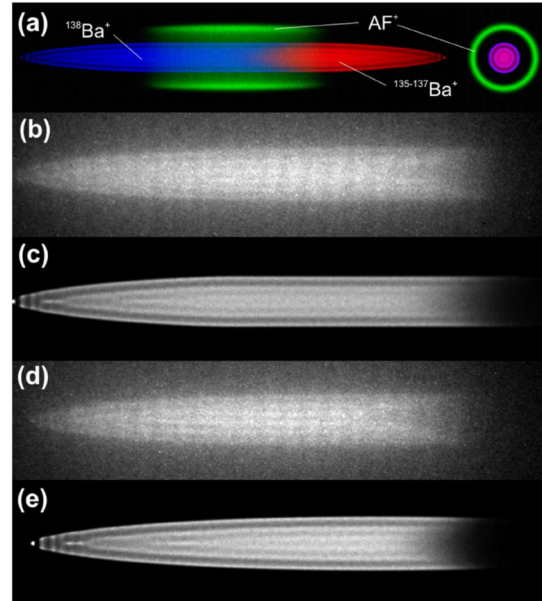


FIG. 1 (color online). (a) Simulated multispecies crystal (side- and cross-sectional views): laser-cooled  $^{138}\text{Ba}^+$  ions (blue) at 25 mK, sympathetically cooled barium isotopes ( $^{135-137}\text{Ba}^+$ , red),  $\text{AF}^+$  ions at 95 mK (green). Lasers propagate to the left. The  $\text{Ba}^+$  ensemble is 1660  $\mu\text{m}$  long and 130  $\mu\text{m}$  in diameter. The  $\text{AF}^+$  sheath is 300  $\mu\text{m}$  in diameter. (b) CCD image of the barium crystal with  $\text{AF}^+$  present; six distinct layers are visible corresponding to three coaxial spheroidal shells (camera exposure time: 0.5 s). (c) Simulation of the crystal in (b). (d) Barium crystal after ejection of all  $\text{AF}^+$  ions. (e) Simulation of the crystal in (d),  $T_{\text{Ba},0} = 20$  mK.

The trapped ions are then extracted by reducing the rf amplitude  $V_0/2$ , which reduces the depth of the trap potential. Heavy and hot ions escape first. Upon leaving the trap, the ions are attracted by the cathode of the channel

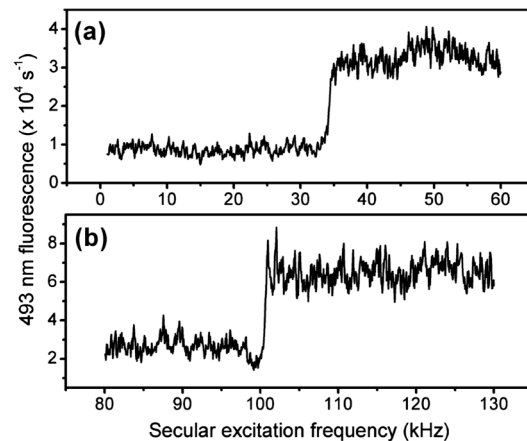


FIG. 2. Mass scan of a Coulomb crystal containing barium and  $\text{AF}^+$  ions. Excitation of radial oscillations of (a)  $\text{AF}^+$  ions and (b)  $\text{Ba}^+$  ions. Calculated single-particle radial secular frequencies are 33.7 kHz and 102 kHz, respectively (respective axial frequencies are at 19.3 and 11.2 kHz).

electron multiplier (CEM). Reducing  $V_0$  from 400 to 150 V removes only the heavy molecules, see Fig. 3. The remaining crystal consists of barium ions only [Fig. 1(d)]. By lowering  $V_0$  further to 0 V this crystal is also ejected and the barium ions are detected, Fig. 3. The ion count peaks occur at clearly separate rf drive amplitudes, confirming that the mass of the trapped molecular ions was roughly 3 times that of barium (i.e.,  $>400$  Da). The ion signal sizes allow determination of the ratio of the number of barium ions to  $\text{AF}^+$  ions (here 5.9:1), assuming equal detection efficiencies. The ion extraction spectrum also provides evidence that the heavier molecules are sympathetically cooled by the barium ions. Figure 3(a) (inset) shows the extraction of both ion species when laser cooling is not applied, i.e., the ensemble is at room temperature due to He buffer gas cooling, while Fig. 3(b) (inset) shows the mass spectrum of an ensemble with similar ion numbers when the barium ions have first been laser-cooled to a cold cloud. Both peaks are clearly narrower in the second case and indicate a narrowed energy distribution for the  $\text{Ba}^+$  and the  $\text{AF}^+$  ions. However, the ion extraction method is not accurate enough to discriminate between a crystal at 25 mK, for example, (Fig. 3), and a cold cloud at a few 100 mK [Fig. 3(b) (inset)].

The ability to image the atomic ion ensemble and the well-defined environment provided by the trap apparatus allows one to deduce further information about the two-species ensemble with the help of molecular dynamics simulations [9,10]. The simulations solve Newton's equation of motion including the effective (i.e., time-averaged), species-dependent trap quasipotential (here, micromotion is neglected), the mutual Coulomb repulsion force between all ions, a light pressure force along the  $z$  direction, and a viscous damping force  $F_D = -\beta v_z$  ( $v_z$  is the  $z$  component of the velocity) representing the laser-cooling process act-

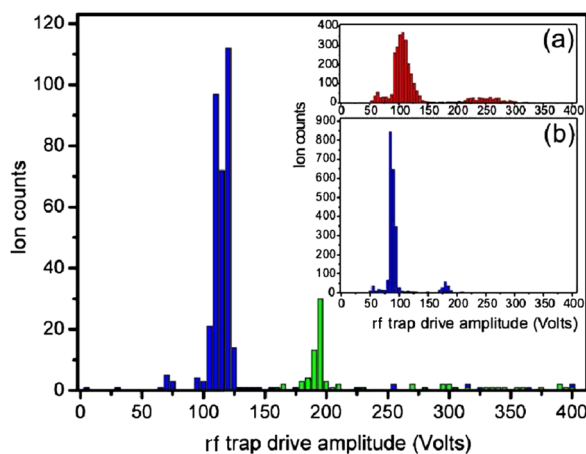


FIG. 3 (color online). Ions (of crystal in Fig. 1) detected on the CEM as the trap rf voltage is decreased. Heavier  $\text{AF}^+$  ions are ejected first (right-hand peak); inset (a) extraction of a different sample of non-laser-cooled barium and  $\text{AF}^+$  ions at  $\sim 300$  K; inset (b) extraction of a laser-cooled cloud at a temperature of a few hundred mK for  $\text{Ba}^+$  and  $\text{AF}^+$  ions.

ing on the  $^{138}\text{Ba}^+$  ions only. The interspecies Coulomb force is responsible for the sympathetic cooling. The damping coefficient  $\beta$  is a (fixed) parameter in the simulations. Heating rates  $H$  (equal for each ion of a given species) are added to the model, each representing the total of all heating effects, examples being: recoil upon photon emission, collisions with residual gas molecules, rf heating (an ion-ion interaction effect in the presence of micromotion [19]), and external electric noise. As a reasonable assumption, we set the heating rate for  $^{138}\text{Ba}^+$  and for the isotopes equal in a given crystal. The heating is implemented by giving each particle a velocity kick proportional to the specified heating rate in a random direction at each time step. Time steps between 50 and 400 ns are used. The competition between the laser cooling and the specified heating rates leads to a steady-state thermal equilibrium. The secular temperature  $T_i$  of each ion species subensemble is defined as  $T_i = \frac{2}{3} \langle \langle E_i \rangle \rangle / k_B$ , where  $\langle \langle E_i \rangle \rangle$  is the time- and subensemble-averaged kinetic energy per ion. The ion velocities follow a Maxwell-Boltzmann distribution.

In addition to the secular (thermal) motion in the quasipotential, micromotion is always present. It occurs essentially in the  $x$ - $y$  plane and contributes to a “blurring” of the crystal images. We have checked the importance of micromotion by performing a simulation taking it fully into account, for the case of an ideal trap. We found that its effects are not dominant for our crystal dimensions and temperatures, i.e., only weakly affect the secular temperature and the image blurring. The micromotion peak-to-peak amplitude orthogonal to the viewing direction is  $\approx 4 \mu\text{m}$  for the radially outermost  $\text{Ba}^+$ , smaller than the resolution of the imaging system,  $\approx 10 \mu\text{m}$ . The corresponding average (radial) micromotion energy per  $\text{Ba}^+$  ion is  $\approx k_B(7.4 \text{ K})$ . For  $\text{AF}^+$  the simulations give a micromotion peak-to-peak amplitude of  $\approx 5 \mu\text{m}$ , corresponding to an average micromotion energy of  $\approx k_B(19 \text{ K})$ . Furthermore, excess micromotion due to trap imperfections could be present. While it was not possible to determine the excess micromotion amplitude, experimentally some trap imperfections were minimized by symmetrizing the crystals via dc offset potentials applied to individual trap electrodes ([10]). The micromotion simulation also indicates that for an ideal trap there is almost no “leakage” of micromotion into the  $z$  direction. Hence, the  $z$  axis would be the preferred laser propagation direction for spectroscopic studies.

By using the quasipotential MD simulations that ignore ion micromotion and its consequent blurring, and by ignoring the finite imaging resolution, the observed blurring of the CCD images is completely ascribed to thermal motion only. Thus, the secular temperature results given below represent upper limits.

Visual comparison of overall structure, structural details, and blurrings of CCD and simulated images permits fitting the number of ions and the heating rates, and thus obtaining the secular temperatures. First, the ion numbers can be

fitted by taking fixed, nominal values for the heating or cooling rates in the simulations, since these quantities are almost uncorrelated. The crystal with  $\text{AF}^+$  present [Fig. 1(b) and 1(c)] contains  $830 \pm 20$   $^{138}\text{Ba}^+$  ions, and  $420 \pm 20$  other isotopes, and, inferred from the ion counter data,  $200 \pm 20$   $\text{AF}^+$ . After removal of  $\text{AF}^+$  [Fig. 1(d) and 1(e)], the  $^{138}\text{Ba}^+$  number was  $770 \pm 20$ , and the isotope number  $410 \pm 20$ , indicating a small loss of ions from the trap during the removal of the  $\text{AF}^+$  ions.

In order to determine the  $\text{AF}^+$  heating rate and temperature via the simulations, the damping coefficient  $\beta$  must be determined directly. We consider the sum of the cooling or heating effects due to the green ( $g$ ) and red ( $r$ ) lasers,  $\beta/m_{\text{Ba}} = 2\sum_i (\hbar k_i^2/2m_{\text{Ba}})\Gamma_i(\partial\rho_e/\partial\Delta_i)|_{\Delta_i}$ . The barium mass  $m_{\text{Ba}}$ , the wave numbers  $k_i$ , and partial decay rates  $\Gamma_i$  for the green and red transitions are constants, while the change in excited state population  $\rho_e$  with laser detunings  $\Delta_i$  is calculated from 8-level Bloch equations using measured laser saturation parameters and detunings [20]. We find  $\beta/m_{\text{Ba}} \approx 760 \text{ s}^{-1}$ , where the dominant cooling effect comes from the green laser. At 20 mK secular temperature, this is equivalent to a cooling rate of  $dT/dt = 2/3(\beta/m_{\text{Ba}})T = 10 \text{ K s}^{-1}$ .

As nonoptimal laser polarizations with respect to the magnetic field and the presence of micromotion may lead to less efficient cooling, we consider a range of  $\beta$  values. For an upper value  $\beta/m_{\text{Ba}} = 870 \text{ s}^{-1}$  we determine the upper limit of the heating rates and the temperatures consistent with the CCD images, and similarly for a minimum value  $\beta/m_{\text{Ba}} = 440 \text{ s}^{-1}$ , we determine the associated lower limit for the heating rates and temperatures. First, the crystal without  $\text{AF}^+$  is simulated, which yields the  $\text{Ba}^+$  heating rate and temperature ( $H_{\text{Ba}^+}, T_{\text{Ba}^+,0}$ ) upper and lower limits (7.6 K/s, 28 mK) and (2.3 K/s, 12 mK), respectively. These heating rates are next used as input to the simulation of the crystal with  $\text{AF}^+$ , since the crystal dimensions are similar. The results are ( $H_{\text{AF}^+}, T_{\text{Ba}^+}, T_{\text{AF}^+}$ ) = (4.3 K/s, 35 mK, 115 mK) and (2.5 K/s, 15 mK, 45 mK), respectively. Figure 1(a) shows the simulation result for an intermediate value  $\beta/m_{\text{Ba}} = 760 \text{ s}^{-1}$ ,  $H_{\text{Ba}^+} = 6.6 \text{ K/s}$ ,  $H_{\text{AF}^+} = 3.7 \text{ K/s}$ , giving  $T_{\text{AF}^+} = 95 \text{ mK}$ . Thus, we find an upper limit of the secular temperature  $T_{\text{AF}^+} = 115 \text{ mK}$ ; this is a conservative estimate in view of the high  $\beta$  value and the neglect of micromotion and of image resolution effects.

The temperature of the molecular ions also depends upon the total ion number. Increasing the number of ions, for example, changes the spatial distribution such that the molecular ions are situated at a larger average distance from the  $\text{Ba}^+$  crystal, leading to a decrease of the sympathetic interaction strength and hence an increase in molecular temperature. Lower temperatures might therefore be possible using smaller  $\text{Ba}^+$  numbers. The simulations also show that the inclusion of an additional ion species with an intermediate mass between that of  $\text{Ba}^+$  and  $\text{AF}^+$ , which would be located radially between the two, would

act as a “conducting layer,” increasing the cooling efficiency and leading to a lower temperature for the heavy molecules. For example, 50 ions of mass 200 Da added to the above crystal would decrease the  $\text{AF}^+$  secular temperature from 95 to 42 mK.

Our method could be extended to heavier molecular ions with multiple positive charges, which can be produced by the ESI source. For a given molecular mass, the higher the charge state, the closer the molecules are to the coolant ions and the more efficient the sympathetic cooling process is. If necessary, exposure of the molecular ions to the cooling lasers could be avoided, by focusing the beams on the atomic coolants only.

The long storage times in the near collisionless environment should permit studies of weak- or low-energy processes, e.g., triplet-singlet decay, photodissociation, vibrational dynamics, black-body-induced processes, and cold collisions. High-resolution spectroscopy could be performed using the method described in [11]. Many experiments could be enhanced by using internally cold or even quantum-state selected molecules, e.g., to allow strongly simplified spectra or quantum-state resolved collision studies. However, since the ion-ion interaction does not couple efficiently to the internal degrees of freedom of the molecules, the internal temperature is expected to be in thermal equilibrium with the vacuum chamber. Cooling the internal degrees of freedom should be possible via radiative cooling in a cryogenic environment.

This work was supported by the DFG program SP1116 and the EC network No. HPRN-CT-2002-00290. We thank H. Wenz and J. Koelemeij for discussions.

- 
- [1] J. Doyle *et al.*, Eur. Phys. J. D **31**, 149 (2004).
  - [2] J.D. Weinstein *et al.*, Nature (London) **395**, 148 (1998).
  - [3] F.M.H. Crompvoets *et al.*, Nature (London) **411**, 174 (2001).
  - [4] T. Rieger *et al.*, Phys. Rev. Lett. **95**, 173002 (2005).
  - [5] M. Wewer and F. Stienkemeier, Phys. Rev. B **67**, 125201 (2003).
  - [6] D.J. Larson *et al.*, Phys. Rev. Lett. **57**, 70 (1986).
  - [7] M.D. Barrett *et al.*, Phys. Rev. A **68**, 042302 (2003).
  - [8] M. Drewsen *et al.*, Phys. Rev. Lett. **93**, 243201 (2004).
  - [9] P. Blythe *et al.*, Phys. Rev. Lett. **95**, 183002 (2005).
  - [10] B. Roth *et al.*, J. Phys. B **38**, 3673 (2005).
  - [11] B. Roth *et al.*, Phys. Rev. A **74**, 040501(R) (2006).
  - [12] A. Kamariotis *et al.*, J. Am. Chem. Soc. **128**, 905 (2006).
  - [13] V.L. Ryjkov *et al.*, Phys. Rev. A **74**, 023401 (2006).
  - [14] M. Yamashita and J.B. Fenn, J. Phys. Chem. **88**, 4451 (1984).
  - [15] I. Waki *et al.*, Phys. Rev. Lett. **68**, 2007 (1992).
  - [16] M.G. Raizen *et al.*, Phys. Rev. A **45**, 6493 (1992).
  - [17] We also trapped rhodamine 101 and 6 G together with laser-cooled barium ions, but both were found to photodissociate in the presence of the cooling lasers.
  - [18] T. Baba and I. Waki, J. Appl. Phys. **92**, 4109 (2002).
  - [19] J.D. Prestage *et al.*, Phys. Rev. Lett. **66**, 2964 (1991).
  - [20] Ch. Raab *et al.*, Phys. Rev. Lett. **85**, 538 (2000).